

Observation of large-scale anisotropy in the arrival directions of cosmic rays with LHAASO-KM2A

Wei Gao^{a,*}, Qing Cao^b, Songzhan Chen^c, Shuwang Cui^b, Huihai He^c, Wenlong Li^a, Sha Wu^c, Hengying Zhang^a and Chengguang Zhu^a on behalf of the LHAASO Collaboration

(a complete list of authors can be found at the end of the proceedings)

^aShandong University, Institute of Frontier and Interdisciplinary Science,
72 Binhai Road, Qingdao 266237, P. R. China

^bHebei Normal University, College of Physics,
20 East. 2nd Ring South Road, Shijiazhuang 050024, P.R.China

^cInstitute of High Energy Physics Chinese Academy of Sciences,
19B Yuquan Road, Beijing 100049, P. R. China

E-mail: gaowei@email.sdu.edu.cn

A global large-scale anisotropy in the arrival directions of cosmic rays were observed both in the Northern and Southern Hemisphere. It is evident that the morphology of the large-scale anisotropy and magnitude is energy dependent. However, only a few experiments can up to PeV with long term data accumulation. The measurement of anisotropy at high energies can provide more clues to the origin and propagation of cosmic rays. The Large High Altitude Air Shower Observatory (LHAASO), covering an area of 1.36 square kilometer, detect cosmic rays from sub-TeV up to 100 PeV with good element discrimination ability. In this paper, data collected by half array of KM2A during 2020 is used to analyze the anisotropy. The anisotropies from 23 TeV up to 985 TeV are reported. The "inverse" anisotropy is observed at 985 TeV with significance of 5σ . The evolution of the anisotropy with energy is consistent with the others. With the operation of LHAASO, more accurate observation for the cosmic-ray anisotropy at higher energy will be made.

*** 37th International Cosmic Ray Conference (ICRC2021), ***

*** 12-23 July 2021 ***

*** Berlin, Germany - Online ***

1. Introduction

The large-scale anisotropy of cosmic rays is an important way to understand origination and propagation of cosmic rays. Through the past few decades, we learn more about the anisotropy from the constantly observations of cosmic-ray experiments. It is evident that the morphology of large-scale anisotropy and the little intensity are energy dependent.

From sub-TeV to tens of TeV, the morphology of anisotropy is dominant by two large-scale features, an excess and deficit feature known as "Tail-in" and "loss-cone". [1] [2] [3]. The amplitude of the first harmonic of the large-scale anisotropy is increasing with the energy and arrival maximum around 10 TeV, and then starts to descend. With the energy increase at sub-PeV and tens of PeV range, the morphology of the large-scale anisotropy change to a new "excess" feature towards the direction of the galactic center and the magnitude increase and then decrease with energy again [4]. The phase change of the large-scale anisotropy might implies that the galactic cosmic-ray sources are densely distributed in the galactic center region. While around the EeV range, the magnitude and direction of the large-scale anisotropy changed again, and the phase change could be an indication as a sign of an extra-galactic origin of ultra-high-energy cosmic rays [5].

Several models attempts to explain the peculiarity of large-scale anisotropy, while the puzzles of large-scale anisotropy are still confused us. We believe that the features of large-scale anisotropy are caused by different origins. To study the large-scale anisotropy at high energy, around "Knee", and in component are important to solve the origin mystery. Due to the extremely small intensity of large-scale anisotropy and low flux of cosmic rays, it is difficult to study at this energy range. However, The Large High Altitude Air Shower Observatory (LHAASO) as a hybrid large array have a wide energy coverage and discrimination ability for particles. That allow us to study the large-scale anisotropy in a wide energy range especially at the high energy. Furthermore, the anisotropy of light and heavy component of cosmic rays around the "Knee" can be also observed to help us to explain the origin of anisotropy. In this work, we provide the preliminary results of the large-scale anisotropy with the half array of LHAASO-KM2A.

2. The LHAASO experiment

LHAASO is a new generation hybrid extensive air shower (EAS) array on Haizi Mountain in Daocheng of Sichuan Province at an altitude of 4400 m above the sea level. LHAASO is expected to explore the origin of high-energy cosmic rays [6] [7]. LHAASO contains three arrays with different types of detectors:

- One square kilometer array (KM2A), contains 5195 ground-based electromagnetic particle detectors (ED) and 1188 underground muon detectors (MD), which has the largest distributed area of 1.3 km² and uniformly distributed;
- Water Cherenkov light detector array (WCDA), which in the central part of LHAASO with low energy threshold is a full coverage array covering total area of 7800 m²;
- Wide field Cherenkov light telescopes array (WFCTA) which is composed of 18 wide field Cherenkov light telescopes (WFCT) that may be distributed flexibly to fit the different physical needs.

The whole array of LHAASO will be completed in this year. The deployed detectors of LHAASO have already on operation. In this paper, we report the large-scale anisotropy observed by the half array of LHAASO-KM2A.

3. Data selection and energy estimation

The data collected by the half array of KM2A during 2020 is used in the analysis. Figure 1 shows the detector layout of half array of KM2A. The data selection is made as the followed criteria:

- the number of triggered ED after noise filter is not less than 20;
- the reconstructed shower core locates in the array (THE area in blue line);
- the zenith angle little than 50 degrees;
- the reconstructed energy, $\log(E_{rec}/GeV)$, should above 3.5.

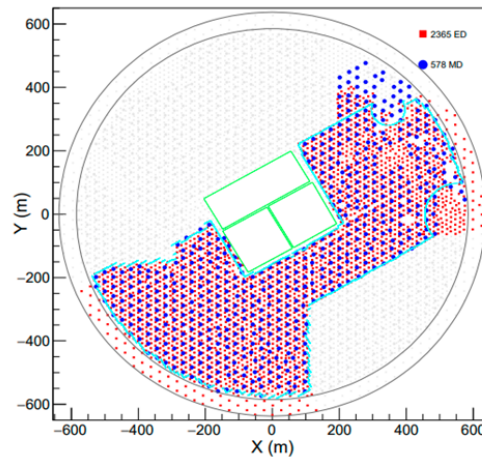


Figure 1: The layout of half array of LHAASO-KM2A [8]

The energy of cosmic rays is estimated by the Monte Carlo simulation. Five groups of dominant component elements, H, He, CNO, MgAlSi, and Fe, are generated according to [9]. The interaction of cosmic rays in the atmosphere is simulated by CORSIKA code with the hadronic interaction model QGSJETII-04 and GHEISHA. About 7.8×10^{10} events are sampled with zenith angle distributed from 0° to 70° and the energy distributed from 1 TeV to 10 PeV. The detector response is simulated with the G4KM2A code based on GEANT-4 [10]. A parameter, $\sqrt{NpE * NuM}$ [11], is used to estimate the primary energy of cosmic rays. NpE is the number of charged particles detected by EDs and the NuM is the sum of muons from MDs. The data sample is divided into four energy intervals according to the reconstructed energy, as table 1 shown. Figure 2 shows the true energy distribution of these four data samples.

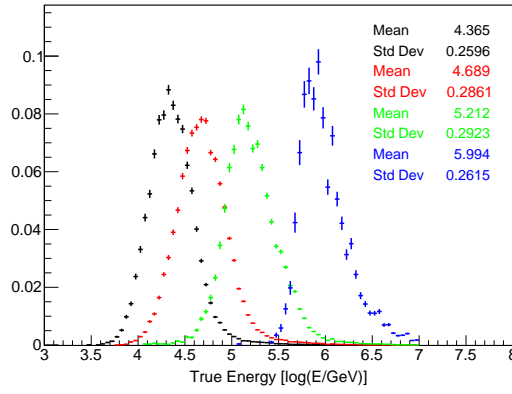


Figure 2: The energy distribution of four intervals.

4. The Results

The large-scale anisotropy in 2020 by half array KM2A is analyzed using the equi-zenith angle method to estimate the background. About 1.56×10^{10} events are remained after the selection with the mean energy about 42 TeV. Plot (a) of Figure 3 shows the significance (top) and intensity (bottom) sky maps, which smooth with 15° radius. The projection of intensity on the right ascension is also provided, as top plot of (b) shown. A spurious frame, anti-sidereal, is used to estimate the systematic error, shown in bottom plot of (b). The typical structures "tail-in" and "loss-cone" are clearly observed and consistent with others.

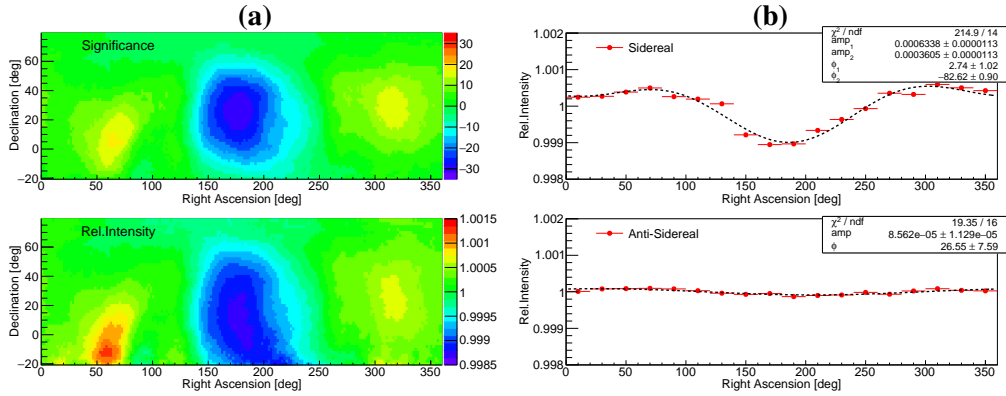


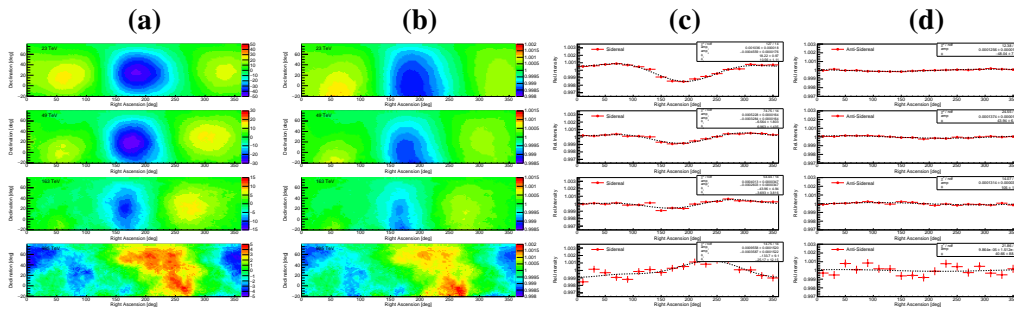
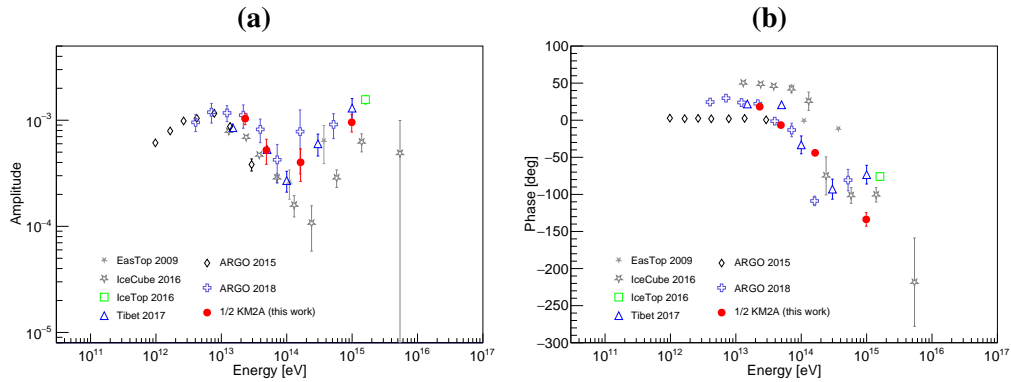
Figure 3: The large-scale anisotropy observed by LHAASO-KM2A

The data sample is divided into four intervals according table 1 to learn the evolution of large-scale anisotropy with energy. Figure 4 shows the observed large-scale anisotropy in four energy intervals with the mean energy of 23, 49, 163 and 985 TeV respectively. Column (a) and (b) are the sky maps of significance and intensity respectively with 30° radius smooth. Plots of column (c) are the projection of intensity of sidereal large-scale anisotropy on right ascension. The magnitude of anti-sidereal distributions shown in column (d) are used to estimate the systematic errors. The amplitudes and phases of first harmonic are listed in the table 1. It is evident that both the amplitude and phase are energy dependent. The highest energy interval is extended to 985 TeV, an "inverse"

Table 1: The amplitude and phase of the first harmonic in four energy intervals

$\log E_{rec}$ (GeV)	E_{mean} (TeV)	Events ($\times 10^8$)	Amp ($\times 10^{-4}$)	σ_{stat} ($\times 10^{-4}$)	σ_{sys} ($\times 10^{-4}$)	ϕ (deg)	σ (deg)
3.50-4.50	23	64.67	10.36	0.180	1.256	18.2	0.97
4.50-5.00	49	73.99	5.23	0.164	1.374	-6.6	1.80
5.00-5.75	163	16.65	4.01	0.347	1.314	-44.0	4.94
≥ 5.75	985	0.86	9.56	1.520	0.986	-133.7	9.10

anisotropy is observed with the significance of 5σ . Figure 5 shows that the results obtained in this work generally consistent with others.


Figure 4: The large-scale anisotropy in four energy intervals.

Figure 5: The evolution of amplitude (a) and phase (b) of large-scale anisotropy with energy by half array of KM2A and other experiments (for details and references see [1][2][3][12][13].)

5. Conclusion

The half array of LHAASO-KM2A have observed the large-scale anisotropy of cosmic rays in a wide energy range from 23 TeV up to 985 TeV with only one year's data. We observed the inversed phase of anisotropy at the high energy of 985 TeV. And the phase reversal process are clearly. The results are consistent with the others. The anisotropy at 985 TeV means that with the

data accumulates LHAASO could measure the sub-PeV up to tens of PeV anisotropy accurately. Furthermore, a study for the component anisotropy of cosmic rays will also be made in the future. These studies will allow us to solve the origin puzzles of anisotropy.

Acknowledgments

This work is supported by the Chinese Postdoctoral Science Foundation (No. 2019M652357), the Natural Sciences Foundation of China (No. U1831129, No. U1931108), the National Key R&D Program of China (No. 2018YFA0404201), the Natural Science Foundation of Shandong Province of China (No.ZR2019MA014) and Young Scholars Program of Shandong University (No.2018WLJH78).

References

- [1] M. G. Aartsen et al., 2016, ApJ, 826, 220
- [2] M. Amenomori et al., 2017, ApJ, 836, 153
- [3] B. Bartoli et al., 2018, ApJ, 861, 93
- [4] D. Kang et al., 2019, PoS(ICRC2019), 306
- [5] The Pierre Auger Collaboration, 2017, Science, 357, 1266
- [6] H. H. He, 2018, Radiat. Detect. Technol. Methods, 2, 1
- [7] Z. Cao et al., 2019, Chin. Astron. Astrophys., 43, 457
- [8] F. Aharonian et al., 2021, Chinese Phys. C, 45, 025002
- [9] T. K. Gaisser et al., 2013, FrPhy, 8, 748
- [10] S. Z. Chen et al., 2019, PoS(ICRC2019), 219
- [11] X. H. Ma et al, 2009, PoS(ICRC2009), 2668
- [12] M. Aglietta et al., 2009, ApJ, 692, 130
- [13] B. Bartoli et al., 2015, ApJ, 809, 90

Full Authors List: LHAASO Collaboration

Zhen Cao^{1,2,3}, F. Aharonian^{4,5}, Q. An^{6,7}, Axikegu⁸, L.X. Bai⁹, Y.X. Bai^{1,3}, L.X. Bai⁹, Y.X. Bai^{1,3}, Y.W. Bao¹⁰, D. Bastieri¹¹, X.J. Bi^{1,2,3}, Y.J. Bi^{1,3}, H. Cai¹², J.T. Cai¹¹, Zhe Cao^{6,7}, J. Chang¹³, J.F. Chang^{1,3,6}, B.M. Chen¹⁴, E.S. Chen^{1,2,3}, J. Chen⁹, Liang Chen^{1,2,3}, Liang Chen¹⁵, Long Chen⁸, M.J. Chen^{1,3}, M.L. Chen^{1,3,6}, Q.H. Chen⁸, S.H. Chen^{1,2,3}, S.Z. Chen^{1,3}, T.L. Chen¹⁶, X.L. Chen^{1,2,3}, Y. Chen¹⁰, N. Cheng^{1,3}, Y.D. Cheng^{1,3}, S.W. Cui¹⁴, X.H. Cui¹⁷, Y.D. Cui¹⁸, B. D’Ettorre Piazzoli¹⁹, B.Z. Dai²⁰, H.L. Dai^{1,3,6}, Z.G. Dai⁷, Danzengluobu¹⁶, D. della Volpe²¹, X.J. Dong^{1,3}, K.K. Duan¹³, J.H. Fan¹¹, Y.Z. Fan¹³, Z.X. Fan^{1,3}, J. Fang²⁰, K. Fang^{1,3}, C.F. Feng²², L. Feng¹³, S.H. Feng^{1,3}, Y.L. Feng¹³, B. Gao^{1,3}, C.D. Gao²², L.Q. Gao^{1,2,3}, Q. Gao¹⁶, W. Gao²², M.M. Ge²⁰, L.S. Geng^{1,3}, G.H. Gong²³, Q.B. Gou^{1,3}, M.H. Gu^{1,3,6}, F.L. Guo¹⁵, J.G. Guo^{1,2,3}, X.L. Guo⁸, Y.Q. Guo^{1,3}, Y.Y. Guo^{1,2,3,13}, Y.A. Han²⁴, H.H. He^{1,2,3}, H.N. He¹³, J.C. He^{1,2,3}, S.L. He¹¹, X.B. He¹⁸, Y. He⁸, M. Heller²¹, Y.K. Hor¹⁸, C. Hou^{1,3}, H.B. Hu^{1,2,3}, S. Hu⁹, S.C. Hu^{1,2,3}, X.J. Hu²³, D.H. Huang⁸, Q.L. Huang^{1,3}, W.H. Huang²², X.T. Huang²², X.Y. Huang¹³, Z.C. Huang⁸, F. Ji^{1,3}, X.L. Ji^{1,3,6}, H.Y. Jia⁸, K. Jiang^{6,7}, Z.J. Jiang²⁰, C. Jin^{1,2,3}, T. Ke^{1,3}, D. Kuleshov²⁵, K. Levochkin²⁵, B.B. Li¹⁴, Cheng Li^{6,7}, Cong Li^{1,3}, F. Li^{1,3,6}, H.B. Li^{1,3}, H.C. Li^{1,3}, H.Y. Li^{7,13}, J. Li^{1,3,6}, K. Li^{3,6}, L. Li²², X.R. Li^{1,3}, Xin Li^{6,7}, Xin Li⁸, Y. Li⁹, Y.Z. Li^{1,2,3}, Zhe Li^{1,3}, Zhuo Li²⁶, E.W. Liang²⁷, Y.F. Liang²⁷, S.J. Lin¹⁸, B. Liu⁷, C. Liu^{1,3}, D. Liu²², H. Liu⁸, H.D. Liu²⁴, J. Liu^{1,3}, J.L. Liu²⁸, J.S. Liu¹⁸, J.Y. Liu^{1,3}, M.Y. Liu¹⁶, R.Y. Liu¹⁰, S.M. Liu⁸, W. Liu^{1,3}, Y. Liu¹¹, Y.N. Liu²³, Z.X. Liu⁹, W.J. Long⁸, R. Lu²⁰, H.K. Lv^{1,3}, B.Q. Ma²⁶, L.L. Ma^{1,3}, X.H. Ma^{1,3}, J.R. Mao²⁹, A. Masood⁸, Z. Min^{1,3}, W. Mitthumsiri³⁰, T. Montaruli²¹, Y.C. Nan²², B.Y. Pang⁸, P. Pattarakijwanich³⁰, Z.Y. Pei¹¹, M.Y. Qi^{1,3}, Y.Q. Qi¹⁴, B.Q. Qiao^{1,3}, J.J. Qin⁷, D. Ruffolo³⁰, V. Rubev²⁵, A. Sáiz³⁰, L. Shao¹⁴, O. Shchegolev^{25,31}, X.D. Sheng^{1,3}, J.Y. Shi^{1,3}, H.C. Song²⁶, Yu.V. Stenkin^{25,31}, V. Stepanov²⁵, Y. Su³², Q.N. Sun⁸, X.N. Sun²⁷, Z.B. Sun³³, P.H.T. Tam¹⁸, Z.B. Tang^{6,7}, W.W. Tian^{2,17}, B.D. Wang^{1,3}, C. Wang³³, H. Wang⁸, H.G. Wang¹¹, J.C. Wang²⁹, J.S. Wang²⁸, L.P. Wang²², L.Y. Wang^{1,3}, R.N. Wang⁸, W. Wang¹⁸, W. Wang¹², X.G. Wang²⁷, X.J. Wang^{1,3}, X.Y. Wang¹⁰, Y. Wang⁸, Y.D. Wang^{1,3}, Y.J. Wang^{1,3}, Y.P. Wang^{1,2,3}, Z.H. Wang⁹, Z.X. Wang²⁰, Zhen Wang²⁸, Zheng Wang^{1,3,6}, D.M. Wei¹³, J.J. Wei¹³, Y.J. Wei^{1,2,3}, T. Wen²⁰, C.Y. Wu^{1,3}, H.R. Wu^{1,3}, S. Wu^{1,3}, W.X. Wu⁸, X.F. Wu¹³, S.Q. Xi^{1,3}, J. Xia^{7,13}, J.J. Xia⁸, G.M. Xiang^{2,15}, D.X. Xiao¹⁶, G. Xiao^{1,3,6}, H.B. Xiao¹¹, G.G. Xin¹², Y.L. Xin⁸, Y. Xing¹⁵, D.L. Xu²⁸, R.X. Xu²⁶, L. Xue²², D.H. Yan²⁹, J.Z. Yan¹³, C.W. Yang⁹, F.F. Yang^{1,3,6}, J.Y. Yang¹⁸, L.L. Yang¹⁸, M.J. Yang^{1,3}, R.Z. Yang⁷, S.B. Yang²⁰, Y.H. Yao⁹, Z.G. Yao^{1,3}, Y.M. Ye²³, L.Q. Yin^{1,3}, N. Yin²², X.H. You^{1,3}, Z.Y. You^{1,2,3}, Y.H. Yu²², Q. Yuan¹³, H.D. Zeng¹³, T.X. Zeng^{1,3,6}, W. Zeng²⁰, Z.K. Zeng^{1,2,3}, M. Zha^{1,3}, X.X. Zhai^{1,3}, B.B. Zhang¹⁰, H.M. Zhang¹⁰, H.Y. Zhang²², J.L. Zhang¹⁷, J.W. Zhang⁹, L.X. Zhang¹¹, Li Zhang²⁰, Lu Zhang¹⁴, P.F. Zhang²⁰, P.P. Zhang¹⁴, R. Zhang^{7,13}, S.R. Zhang¹⁴, S.S. Zhang^{1,3}, X. Zhang¹⁰, X.P. Zhang^{1,3}, Y.F. Zhang⁸, Y.L. Zhang^{1,3}, Yi Zhang^{1,3}, Yong Zhang^{1,3}, B. Zhao⁸, J. Zhao^{1,3}, L. Zhao^{6,7}, L.Z. Zhao¹⁴, S.P. Zhao^{13,22}, F. Zheng³³, Y. Zheng⁸, B. Zhou^{1,3}, H. Zhou²⁸, J.N. Zhou¹⁵, P. Zhou¹⁰, R. Zhou⁹, X.X. Zhou⁸, C.G. Zhu²², F.R. Zhu⁸, H. Zhu¹⁷, K.J. Zhu^{1,2,3,6} and X. Zuo^{1,3}

¹Key Laboratory of Particle Astrophysics & Experimental Physics Division & Computing Center, Institute of High Energy Physics, Chinese Academy of Sciences, 100049 Beijing, China.

²University of Chinese Academy of Sciences, 100049 Beijing, China.

³TIANFU Cosmic Ray Research Center, Chengdu, Sichuan, China.

⁴Dublin Institute for Advanced Studies, 31 Fitzwilliam Place, 2 Dublin, Ireland.

⁵Max-Planck-Institut für Nuclear Physics, P.O. Box 103980, 69029 Heidelberg, Germany.

⁶State Key Laboratory of Particle Detection and Electronics, China.

⁷University of Science and Technology of China, 230026 Hefei, Anhui, China.

⁸School of Physical Science and Technology & School of Information Science and Technology, Southwest Jiaotong University, 610031 Chengdu, Sichuan, China.

⁹College of Physics, Sichuan University, 610065 Chengdu, Sichuan, China.

¹⁰School of Astronomy and Space Science, Nanjing University, 210023 Nanjing, Jiangsu, China.

¹¹Center for Astrophysics, Guangzhou University, 510006 Guangzhou, Guangdong, China.

¹²School of Physics and Technology, Wuhan University, 430072 Wuhan, Hubei, China.

¹³Key Laboratory of Dark Matter and Space Astronomy, Purple Mountain Observatory, Chinese Academy of Sciences, 210023 Nanjing, Jiangsu, China.

¹⁴Hebei Normal University, 050024 Shijiazhuang, Hebei, China.

¹⁵Key Laboratory for Research in Galaxies and Cosmology, Shanghai Astronomical Observatory, Chinese Academy of Sciences, 200030 Shanghai, China.

¹⁶Key Laboratory of Cosmic Rays (Tibet University), Ministry of Education, 850000 Lhasa, Tibet, China.

¹⁷National Astronomical Observatories, Chinese Academy of Sciences, 100101 Beijing, China.

¹⁸School of Physics and Astronomy & School of Physics (Guangzhou), Sun Yat-sen University, 519000 Zhuhai, Guangdong, China.

¹⁹Dipartimento di Fisica dell’Università di Napoli ‘Federico II’, Complesso Universitario di Monte Sant’Angelo, via Cinthia, 80126 Napoli, Italy.

²⁰School of Physics and Astronomy, Yunnan University, 650091 Kunming, Yunnan, China.

²¹D’epartement de Physique Nucléaire et Corpusculaire, Faculté de Sciences, Université de Genève, 24 Quai Ernest Ansermet, 1211 Geneva, Switzerland.

²²Institute of Frontier and Interdisciplinary Science, Shandong University, 266237 Qingdao, Shandong, China.

²³Department of Engineering Physics, Tsinghua University, 100084 Beijing, China.

²⁴School of Physics and Microelectronics, Zhengzhou University, 450001 Zhengzhou, Henan, China.

²⁵Institute for Nuclear Research of Russian Academy of Sciences, 117312 Moscow, Russia.

²⁶School of Physics, Peking University, 100871 Beijing, China.

²⁷School of Physical Science and Technology, Guangxi University, 530004 Nanning, Guangxi, China.

²⁸Tsung-Dao Lee Institute & School of Physics and Astronomy, Shanghai Jiao Tong University, 200240 Shanghai, China.

²⁹Yunnan Observatories, Chinese Academy of Sciences, 650216 Kunming, Yunnan, China.

³⁰Department of Physics, Faculty of Science, Mahidol University, 10400 Bangkok, Thailand.

³¹Moscow Institute of Physics and Technology, 141700 Moscow, Russia.

³²Key Laboratory of Radio Astronomy, Purple Mountain Observatory, Chinese Academy of Sciences, 210023 Nanjing, Jiangsu, China.

³³National Space Science Center, Chinese Academy of Sciences, 100190 Beijing, China.